AGU PUBLICATIONS

Geophysical Research Letters

RESEARCH LETTER
10.1002/2014GL062121

Key Points:
- Producing the modern cratering record on Venus requires two types of volcanism
- Thin, morphologically similar flows dominate and tall volcanoes are secondary
- Noncatastrophic processes can explain the distribution of modified craters

Correspondence to:
J. G. O'Rourke,
jorourke@caltech.edu

Citation:
O'Rourke, J. G., A. S. Wolf, and B. L. Ehlmann (2014), Venus: Interpreting the spatial distribution of volcanically modified craters, *Geophys. Res. Lett.*, *41*, 8252–5260, doi:10.1002/2014GL062121.

Received 7 OCT 2014
Accepted 21 NOV 2014
Accepted article online 26 NOV 2014
Published online 11 DEC 2014

Venus: Interpreting the spatial distribution of volcanically modified craters

Joseph G. O'Rourke[1], Aaron S. Wolf[2], and Bethany L. Ehlmann[1,3]

[1]Division of Geological and Planetary Sciences, California Institute of Technology, Pasadena, California, USA, [2]Department of Earth and Environmental Sciences, University of Michigan, Ann Arbor, Michigan, USA, [3]Jet Propulsion Laboratory, Pasadena, California, USA

Abstract To understand the impact cratering record on Venus, we investigate two distinct resurfacing styles: localized, thin flows and large shield volcanoes. We statistically analyze the size-frequency distribution of volcanically modified craters and, using Monte Carlo simulations, their spatial distribution. Lava flows partially fill most craters, darkening their floors in radar images. We find that a model featuring localized, thin flows occurring throughout geologic time predicts their observed distribution. Individual flows may be morphologically indistinguishable, but, combined, they cover large provinces. Recent mantle plumes may drive a small amount of hot spot magmatism that produces the observed clusters of large shield volcanoes and obviously embayed craters. Ultimately, our analysis demonstrates that two styles of volcanism are needed to explain the observed properties of impact craters and that catastrophic resurfacing is not required.

1. Introduction

Venus and Earth are terrestrial planets with similar sizes, densities, and positions in the solar system. They are usually assumed to have similar bulk compositions too [e.g., *Namiki and Solomon*, 1998]. But Earth is clement, whereas greenhouse gases have raised surface temperatures on Venus to ~740 K [e.g., *Bullock and Grinspoon*, 2001]. Differences in the mantle dynamics between these planets mirror, and probably explain, their distinctive surface conditions. On Earth, plate tectonics recycles surface material, concentrates volcanism near spreading centers and subduction zones, and sustains habitability [e.g., *Korenaga*, 2012]. Venus, in contrast, currently operates in the stagnant-lid regime—the mode of mantle convection found on every terrestrial planet except Earth [e.g., *Solomatov and Moresi*, 1996, 2000]—where solid-state convection occurs below an unbroken, planet-encompassing lithosphere. Beyond this simple description of its present state, the history of Venus is vigorously debated.

A global stratigraphy for the surface of Venus has been proposed, corresponding to a so-called "directional" evolution. Spatially disparate terrains are grouped into global units based on morphologic similarities [e.g., *Basilevsky and Head*, 1998, 2000, 2002; *Ivanov and Head*, 2011, 2013]. A relative age is assigned to each unit with crater counting, which relies on virtually all craters residing atop the local stratigraphy. Each unit is then attributed to volcanic and/or tectonic processes. The key feature of the directional history is that these processes are global and basically confined to the time period that their associated units represent. For example, global tectonism is interpreted to have shaped the oldest tessera terrain and heavily tectonized volcanic plains, but its intensity quickly diminished during the formation of the younger volcanic plains. Transitions between different global processes are rapid in this history. The emplacement of volcanic plains and features covering most of Venus, in particular, is proposed to have lasted ~100 Myr, less than half of the mean surface age [e.g., *Schaber et al.*, 1992]. Several geophysical explanations have emerged for this catastrophic resurfacing event [e.g., *Turcotte*, 1993; *Moresi and Solomatov*, 1998; *Reese et al.*, 1999; *Armann and Tackley*, 2012].

Countervailing evidence suggests that the surface evolution of Venus was likely more complex. New mapping efforts indicate that large areas preserve an ancient history that records the effects of localized resurfacing processes that operated throughout geologic time [e.g., *Guest and Stofan*, 1999; *Stofan et al.*, 2005; *Hansen and Lopez*, 2010]. Similar-looking terrains scattered across Venus are not always temporally correlated [e.g., *Guest and Stofan*, 1999]. Feedback between atmospheric conditions and interior dynamics might cause localized resurfacing and strong variations in surface age [*Noack et al.*, 2012].

Without the necessity of catastrophic resurfacing, modelers might also stick to the simplest story for mantle dynamics—continual evolution in the stagnant-lid regime, which is most natural for terrestrial planets lacking surface water [e.g., *Solomatov*, 1995; *Korenaga*, 2010; *O'Rourke and Korenaga*, 2012].

Observations of impact craters constrain the geologic history of Venus. In the early 1990s, synthetic aperture radar images from NASA's Magellan mission, covering ~98% of the surface, revealed ~1000 craters [*Phillips et al.*, 1992; *Schaber et al.*, 1992]. Considering the abundance of likely impactors and the strength of atmospheric screening, the effective mean surface age is ~300 Myr to 1 Gyr [*McKinnon et al.*, 1997]. Slow winds and the absence of surface water preclude the erosion of craters, although eolian processes may degrade associated features like dark haloes and parabolic ejecta deposits over time [*Izenberg et al.*, 1994; *Basilevsky and Head*, 2002]. Only a small percentage (<10%) of the extant craters are obviously embayed by external lava flows that breach their rims or cover a large portion of their ejecta blankets [*Schaber et al.*, 1992; *Phillips et al.*, 1992; *Strom et al.*, 1994; *Collins et al.*, 1999]. Coupled with the apparent statistical randomness of the coordinates of craters, this observation was initially seen as strong evidence for catastrophic resurfacing and a relatively young, superimposed crater population. Adherents to catastrophic resurfacing invoke ~0.01–0.15 km^3/yr of subsequent, more recent volcanism to explain the obviously embayed craters [e.g., *Strom et al.*, 1994].

However, there are challenges to this paradigm. Crater locations are not necessarily random with respect to geology [e.g., *Hauck et al.*, 1998] or topography [e.g., *Herrick and Phillips*, 1994]. Localized resurfacing events that occur frequently over several Gyr can also yield an overall spatial distribution that looks random [e.g., *Phillips et al.*, 1992]. *Bjonnes et al.* [2012] produced a low number of embayed craters in Monte Carlo simulations featuring shield volcanoes—but did not investigate their spatial distribution. They assumed that all craters not obviously embayed in Magellan imagery are pristine.

A growing body of evidence suggests that thin, morphologically indistinguishable lava flows have filled the radar-dark craters, which comprise ~80% of the total population. The floors of these craters have low radar backscatter relative to their ejecta blankets and rims—they thus resemble the volcanic plains. Neither impact melting nor eolian processes fully account for their morphological differences with the bright-floored craters, which appear truly pristine [*Wichman*, 1999; *Herrick and Sharpton*, 2000; *Herrick and Rumpf*, 2011]. In particular, dark-floored craters have systematically shallower rim-floor depths and rim heights than bright-floored craters, implying partial filling of these craters and flooding of their surroundings. Additionally, virtually all dark-floored craters with $D > 20$ km and dark halos surrounding continuous ejecta have had a portion of their dark halo removed [*Herrick and Rumpf*, 2011]. *Ivanov and Head* [2013] compared the possible magmatic filling of dark-floored craters to the subtle embayment by mare material of Lichtenberg, a rayed crater on the Moon [*Schultz and Spudis*, 1983]. Interior floor volcanism may also contribute to crater filling. Age estimates that underlie the directional stratigraphy are invalid if most craters suffered postimpact volcanic modification. Until now, no study has attempted to simulate the volcanic modification of dark-floored craters.

Here we test two noncatastrophic models for volcanic processes: thin, low viscosity flows and large shield volcanoes. We compare predictions for the spatial and size-frequency distributions of volcanically modified craters against observations. We find that no single process can explain the cratering record, but thin flows are likely responsible for most magmatism. This implies that catastrophic resurfacing need not be invoked; rather, stagnant-lid convection fed localized volcanism continuously throughout time.

2. Crater Classifications and Size-Frequency Distributions

Two different databases of impact craters are available, hosted by the Lunar and Planetary Institute (LPI) [*Herrick et al.*, 1997] and the U.S. Geological Survey (USGS) Astrogeology Branch [*Schaber et al.*, 1992; *Strom et al.*, 1994]. We primarily rely on the LPI database, which contains detailed, quantitative descriptions of crater morphology and does not bias its classifications with assumptions about the geologic history of Venus. Figure 1 contains our map of impact craters. We are interested in the location, diameter, floor reflectivity, and any obvious embayment by external lava flows of each crater. Out of 933, 748 (~80%, filled symbols) are classified as dark-floored and the remaining 185 (~20%, unfilled symbols) are radar-bright. Only 86 craters (~9%, red symbols) show unequivocal signs of external embayment. Merely six obviously embayed craters also have radar-bright floors.

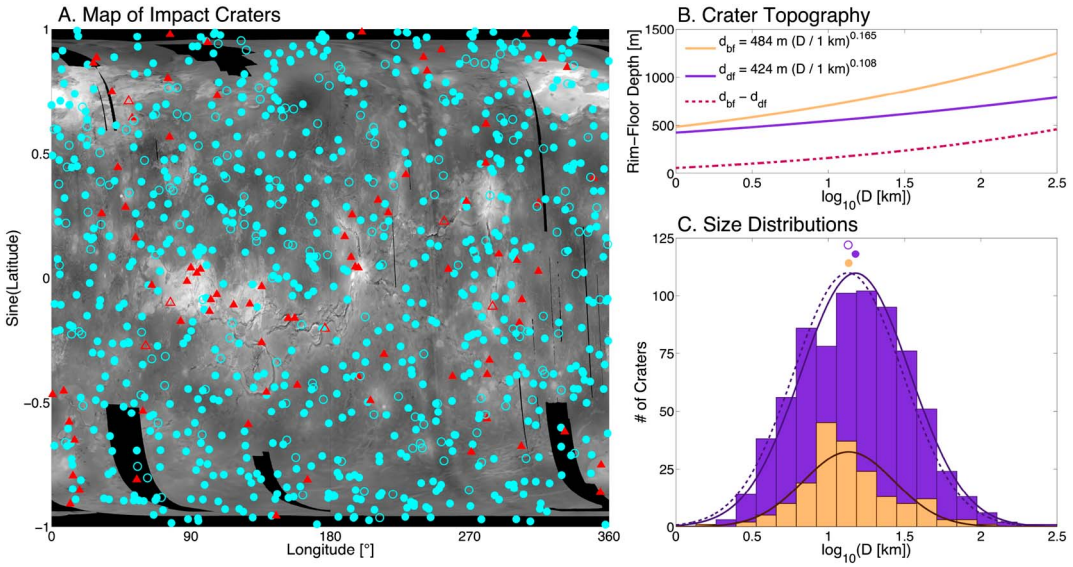

Figure 1. (a) Map of impact craters on Venus based on the LPI database [*Herrick et al.*, 1997]. Locations of 933 craters are plotted over the available Magellan topography (elevated terrain is brighter). The 847 craters without exterior volcanic embayment are blue circles, whereas the 86 embayed craters are red triangles. Filled symbols represent the 748 craters with radar-dark floors, whereas symbols for the 185 bright-floored craters are unfilled. (b) Best fit formulas from *Herrick and Rumpf* [2011] for the rim-floor depths of bright-floored (d_{bf}) and dark-floored (d_{df}) craters and their difference. (c) Histograms showing the distributions of the diameters of dark-floored (purple) and bright-floored (orange) craters, along with their best fit normal probability density functions (pdfs, solid curves). The dashed, purple curve is a pdf that approximates the size-frequency distribution of craters that were volcanically modified to produce the dark-floored ones (inferred as discussed in section 4). The mean value of this pdf (empty, purple circle) is nearly identical to the average diameter of the bright-floored craters.

Eleven craters are incompletely described in the LPI database because of gaps in the Magellan imagery of their floors and rims. Following the USGS database, we classify the craters Ellen and Orlova as dark-floored and, respectively, as obviously embayed and not. We exclude the remaining nine craters from our analysis. We also analyze the distribution of 56 (~6%) obviously embayed craters in the USGS database. However, only 32 of these craters are similarly classified in the LPI database. The rest do not have distinct breaches in their rims or ejecta blankets, and some small craters are omitted entirely.

A complex interplay between the impactor population, atmospheric screening, and volcanic modification creates the modern size-frequency distribution of craters. Overall, observed diameters range from ~1.5 to 268.7 km, with a median of 14.5 km. Larger craters are deeper, as seen in Figure 1b, which contains formulas for the rim-floor depths of dark- and bright-floored craters (d_{df} and d_{bf}, respectively) that were fit to topographic profiles of 91 craters with $D > 15$ km [*Herrick and Rumpf*, 2011]. Volcanically modified craters tend to be larger than unmodified ones. Craters that are and are not obviously embayed have median diameters of 23.6 and 20.2 km, respectively. Likewise, the median diameter of dark-floored craters is 21.3 km, compared to 17.6 km for the bright-floored ones. Figure 1c shows the two size-frequency distributions (histograms), along with best fit lognormal probability density functions (pdfs, solid curves). The best fit parameters in log space are $\mu_b = 1.133$ and $\sigma_b = 0.3$ for bright-floored craters and $\mu_d = 1.178$ and $\sigma_d = 0.358$ for dark-floored craters. We assessed uncertainties on these distributions using standard bootstrap Monte Carlo resampling, yielding errors on the mean log diameters of 0.006 and 0.004, respectively, compared to $\mu_d - \mu_b = 0.045$. Thus, the difference between these two pdfs is statistically significant.

3. Quantifying Randomness of Spatial Distributions

We analyze the populations of craters on Venus using nearest neighbor distances [*Hauck et al.*, 1998]. This method is more sensitive than chi-squared tests on coordinates and intercrater angles. Given coordinates

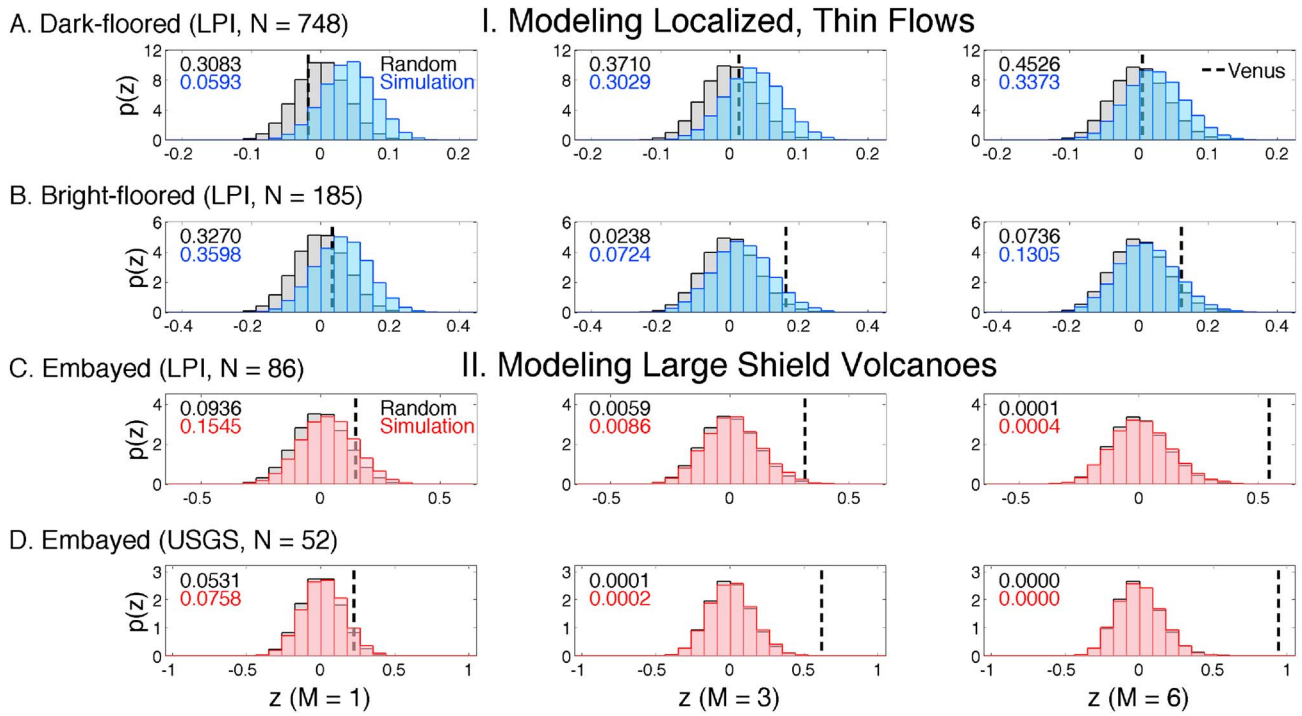

Figure 2. Comparisons of test statistics representing the distributions of four populations of craters (vertical, dashed lines) to distributions of test statistics associated with 10^5 sets of randomly distributed points (grey histograms) and 10^4 simulations (colored histograms). From left to right, each column shows values of z for $M = 1$, 3, and 6. One-sided p values for testing the hypotheses that the spatial distributions on Venus are random (black, upper) or result from the simulated processes (colored, lower) are reported in the top, left corner of each plot. Simulations of resurfacing by thin flows (blue histograms) successfully reproduce the distributions of the (a) dark-floored and (b) bright-floored craters in the LPI database. Simulations in which large shield volcanoes are produced everywhere on Venus with equal probability (red histograms) fail to reproduce the clustering of obviously embayed craters in both (c) the LPI and (d) USGS databases.

for N craters, we can calculate sets of angular distances between each crater and its Mth nearest neighbors. As noted by *Scott and Tout* [1989], the pdf for randomly distributed craters is given by

$$p(\theta|N,M) = \frac{(N-1)!}{2^{N-1}(N-M-1)!(M-1)!}\sin(\theta)[1-\cos(\theta)]^{M-1}[1+\cos(\theta)]^{N-M-1}, \quad (1)$$

where $\theta \in [0,\pi]$. *Hauck et al.* [1998] used a pdf for the $M = 1$ case based on modeling the spatial crater distribution as a Poisson process describing points placed randomly on a plane, but their formula diverges slightly from the correct pdf for $N < 10^3$ because of the difference between arc and chord lengths. We calculate the first and second moments of the above pdf, representing the expected mean angular distance and its corresponding standard deviation, μ_{exp} and σ_{exp}, respectively. We then compare the expected value to the observed mean angular distance for the true crater population, μ_{obs}, using the normalized test statistic [*Hauck et al.*, 1998]:

$$z = \frac{\mu_{exp} - \mu_{obs}}{\sigma_{exp}}. \quad (2)$$

For a perfectly random distribution, $z = 0$, reflecting points that show a small random degree of clustering. Distributions with values of $z < 0$ or $z > 0$ reflect underclustering or overclustering of points, respectively.

We explored the spatial distributions of dark- and bright-floored craters, along with obviously embayed craters from both databases. The z statistic values for each population with $M = 1$, 3, and 6 were calculated and are shown as dashed, vertical lines in Figure 2. For comparison, we computed distributions of z with 10^5 random placements of points on a sphere (grey histograms in Figure 2). At each value of M, we calculated one-sided p values to test the hypothesis of random spatial distribution for each population, where values of $p \leq 0.01$–0.05 are considered sufficiently unlikely to reject the corresponding null hypothesis.

We find that the distributions of dark- and bright-floored craters are compatible with randomness (shown by comfortably large p values), although bright-floored craters perhaps indicate some degree of clustering

for $M \geq 3$. Obviously embayed craters are consistent with random distributions for $M = 1$ but are unambiguously clustered for $M \geq 3$, as shown in the lower half of Figure 1. Those in the LPI database are slightly less clustered than those in the USGS database, which includes very few obviously embayed craters on volcanic plains.

4. Modeling Localized, Thin Flows on Venus

We test whether localized resurfacing can reproduce the observed cratering record using Monte Carlo simulations. Computational and conceptual expedience mandate several simplifying assumptions. In particular, we assume equal diameters for all craters and model cratering as a Poisson process that occurs everywhere on the surface with equal probability. We simulate cratering events with an exponential distribution, using a time constant, τ_c, that is fixed for the total duration of each simulation, T. Likewise, we model resurfacing events as a Poisson process with another time constant, τ_r. We use $T = 3.0$ Gyr for all simulations, although we obtain consistent results for $T \leq 4.5$ Gyr. Assumptions of constant rates for cratering and resurfacing are ill-suited to early Venus, which endured giant impacts, a solidifying magma ocean, and the Late Heavy Bombardment [e.g., *Agnor et al.*, 1999; *Solomatov and Moresi*, 2000]. Nevertheless, the resulting distributions are somewhat insensitive to this simplification because more recent resurfacing has erased the surface record of this ancient period.

Using the general simulation method described above, we explore a number of resurfacing models to determine how well they can reproduce the observed crater distributions. Our first task is to investigate whether localized, thin flows can reproduce the populations of dark- and bright-floored craters. We developed a simple model for this type of magmatism, shown in the left side of Figure 3. Here craters within R_p of the center of the resurfacing event are partially filled and should have radar-dark floors. Lava can breach crater rims on short length scales or emerge from fractures on crater floors. Once filled X times, craters are completely buried and thus erased from the surface record. Craters that were never partially filled should appear radar-bright today. Figure 3 contains examples of each type of crater. Each lava flow covers a fraction of the surface, $\alpha = 0.25(R_p/R_V)^2$, where $R_V \approx 6052$ km is the radius of Venus. For $X = 5$, implied flow depths are ~150 m. We model each flow as one instantaneous event, but, in reality, multiple smaller flows from a single source region could combine over a few Myr. With the initial condition of zero craters at the start of each simulation, we calculate the expected number of craters that have experienced x resurfacing events by solving a system of differential equations:

$$\frac{dN_0(t)}{dt} = \frac{1}{\tau_c} - \frac{\alpha N_0(t)}{\tau_r} \tag{3}$$

$$\frac{dN_x(t)}{dt} = \frac{\alpha}{\tau_r}[N_{x-1}(t) - N_x(t)], \tag{4}$$

where $0 < x < X$. Specifically, we can calculate the expected number of bright-floored craters as a function of time, defined as those that have experienced no resurfacing events ($x = 0$):

$$N_b(t) = \frac{\tau_r}{\alpha\tau_c}\left[1 - \exp\left(-\frac{\alpha t}{\tau_r}\right)\right]. \tag{5}$$

Likewise, we can predict how many craters have experienced $x > 0$ partial resurfacing events:

$$N_x(t) = N_b(t) - \left\{\sum_{i=1}^{x}\left[\frac{\alpha^{(i-1)}t^i}{i!\tau_r^{(i-1)}\tau_c^i}\right]\right\}\exp\left(-\frac{\alpha t}{\tau_r}\right). \tag{6}$$

The total number of dark-floored craters is given simply by $N_d(t) = N_1(t) + \cdots + N_{X-1}(t)$. For realistic evolution times of ~3 Gyr, $t \gg \tau_r/\alpha$ and thus the simulation reaches equilibrium with $N_x = N_b$ and $N_d/N_b = X - 1$. We can therefore predict the expected number of bright- and dark-floored craters that will remain at the end of a simulation for any choice of X, R_p, τ_r, and τ_c. We used $\tau_c = 1$ Myr/event, well within the range of plausible estimates [*McKinnon et al.*, 1997]. With this cratering rate, a catastrophically resurfaced Venus would have a mean surface age of 933 Myr. A larger or smaller τ_c simply implies that τ_r should proportionally increase or decrease to maintain the observed number of craters. We tested several pairs of values for α and τ_r.

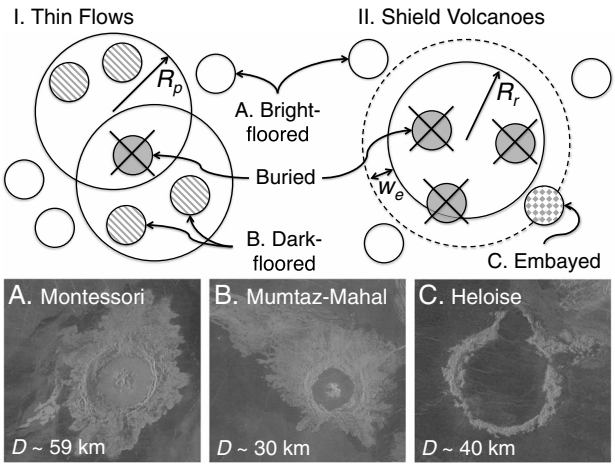

Figure 3. Cartoons of our two models of volcanic resurfacing events and Magellan radar images of representative craters. Initially, craters are bright-floored and pristine like Montessori. (left) Thin, low viscosity flows partially bury craters within a radius R_p, which become dark-floored like Mumtaz-Mahal. Craters that are filled X times are completely buried. In this cartoon, $X = 2$, but we ran simulations with $X = 2$–5. (right) Large shield volcanos completely bury all impact craters within a radius R_r. Craters on the outskirts, in an annulus of width w_e, are partially embayed like Heloise.

Representative results from 10^4 simulations are plotted as blue histograms in Figure 2. In this case, we set $X = 5$, $\tau_r = 0.1$ Myr/event, and $R_p = 280$ km ($\alpha = 10^{-3.27}$), which yields $N_b(T) = 187 \pm 18$ and $N_d(T) = 744 \pm 28$. All p values are >0.05, meaning that the observed distribution of dark- and bright-floored craters represents a statistically plausible outcome of our model. The mean age of craters that survive to the present is 562 Myr, but craters as old as ~2 Gyr occasionally survive. The mean age of the most recent partial fillings of each dark-floored crater is 190 Myr. So although much of the surface is young within this model, Venus should preserve an ancient history in many locations. Bright-floored craters should have a variety of ages, consistent with the observation that some bright-floored craters (presumably the younger ones) have parabolic deposits, while many others do not [e.g., *Herrick et al.*, 1997].

The suitability of this resurfacing model is largely insensitive to our choice of simulation parameters. Specifically, we obtained consistent results for $\tau_r \leq 1.5$ Myr/event and corresponding $R_p \leq 1079$ km ($\alpha \leq 10^{-2.1}$). For $X \leq 4$, the fraction of bright-floored craters increases beyond what is currently observed, but simulations still reproduce the observed distributions of dark- and bright-floored craters. As τ_r increases, both groups of craters become increasingly clustered. That is, p values for the bright-floored craters increase (to >0.3), but the match to the $M = 1$ case for dark-floored craters worsens.

We considered whether this model is consistent with the differences between the size-frequency distributions of dark- and bright-floored craters. The probability of observing a crater with diameter D is $p(D) = p(D|I,A)p(D|V)$, where $p(D|I,A)$ is the probability of crater production given the impactor population and the effects of atmospheric screening, represented by I and A, respectively. In this model, the probability that a produced crater escapes complete volcanic burial until the present is directly proportional to its original depth, $p(D|V) \propto d(D)$. Diameter is only important to survival insofar as it predicts depth because it is much smaller than the length scale of a typical flow. Assuming that all craters were originally as deep as the bright-floored ones are today, we can approximate the diameter-depth relation, $d(D) \sim d_{\mathrm{bf}}(D)$. We calculated the initial size-frequency distribution of craters that were modified to produce the observed dark-floored craters, $p_d(D|I,A) \propto p_d(D)/d_{\mathrm{bf}}(D)$, where $p_d(D)$ is the pdf associated with the size-frequency distribution of dark-floored craters. We plotted $p_d(D|I,A)$, renormalized, as a dashed, purple curve in Figure 1c. This derived pdf has a mean value that agrees with that of the bright-floored craters to within derived uncertainties, i.e., $\Delta\mu < 0.004$. The size-frequency distribution of impactors and the efficiency of atmospheric screening may have varied over Venus history; nevertheless, this correspondence suggests that the dark-floored craters derived from a population like the bright-floored craters, modified by a depth-dependent process like thin flows.

5. Shield Volcanoes and Clustering of Embayed Craters

Simulations of the evolution of the surface of Venus usually only consider volcanic modification of obviously embayed craters by large shield volcanoes. The right side of Figure 3 is a cartoon of the model used in previous Monte Carlo simulations [e.g., *Strom et al.*, 1994; *Bjonnes et al.*, 2012]. Craters are completely obliterated within a circular patch of radius R_r, which covers a fraction of the surface, $\alpha = 0.25(R_r/R_V)^2$.

Within the external annulus of width w_e, craters are partially embayed. If we again assume that cratering and resurfacing are Poisson processes that occur everywhere on the surface with equal probability, then the expected number of craters exposed on the surface as a function of time, $N(t)$, equals $N_b(t)$ from equation (5). This model becomes degenerate with our model for thin-flow magmatism in the case that $X = 1$, $R_r \rightarrow 0$, and $w_e \rightarrow R_p$ but represents a distinct volcanic process in which a single source of magma feeds the growth of a shield volcano that is identifiable in the Magellan imagery.

Strom et al. [1994] claimed that any noncatastrophic model must use extremely low values of α ($\leq 3 \times 10^{-4}$) because they believed that Venus lacks volcanic features covering 0.03–10% of the surface [*Head et al.*, 1992; *Crumpler et al.*, 1997]. They argued that such models inevitably produce too many embayed craters. However, mappers might mistakingly lump several distinct lava flows together as one based on the available data, lacking mineralogical information or high-resolution imagery. *Bjonnes et al.* [2012] found that noncatastrophic models using larger resurfacing patches ($\alpha = 0.001$–0.01) can produce a random-looking distribution of craters with a low number of partially embayed craters.

Tuning this model to obtain the observed number of embayed craters is easy, provided that the external annulus w_e is sufficiently small. However, some values of w_e are perhaps more physically plausible than others. *Bjonnes et al.* [2012] used the median diameter of observed craters (~15 km), while *Strom et al.* [1994] used the observed diameters of craters as a distribution of values for w_e. Other authors model volcanoes as pyramids with slopes ~0.2–2.0° [e.g., *Romeo*, 2013]. A typical crater with diameter $D = 15$ km might have a rim-floor depth of ~750 m and a rim height of ~210 m [*Herrick and Rumpf*, 2011]. In this scenario, $w_e \sim 15$–150 km is the region where lava is thick enough to flow over the rim but too thin to completely fill the crater and bury the rim. Larger craters are more likely to intersect this region, so it is not surprising that obviously embayed craters tend to be larger than average.

Resurfacing models featuring only large shield volcanoes, however, always fail to reproduce the observed clustering of embayed craters on Venus. We performed simulations using virtually the same parameters as *Bjonnes et al.* [2012]. Specifically, we set $\tau_c = 1$ Myr/event and $\alpha = 10^{-3}$. We found that $\tau_r = 0.9898$ Myr/event produces $N(T) = 942 \pm 36$. We ran two sets of 10^4 simulations each for $w_e = 13.9$ and 21.8 km, which yield 56 ± 8 and 86 ± 9 embayed craters, respectively, for comparison to the LPI and USGS databases. Our results are plotted as red histograms in Figure 2. These simulations predict a random distribution of obviously embayed craters, which is incompatible with reality. Large shield volcanoes can only produce the observed clustering if they are restricted to a few regions on Venus.

Our conclusion here is again insensitive to our choice of simulation parameters. In particular, we tested different values of T and the extreme case where resurfacing is halted ~1.5 Gyr before the end of the simulations, which allows the overall distribution to look random for $\alpha \leq 10^{-2}$ [*Bjonnes et al.*, 2012]. But we found that embayed craters are always insufficiently clustered ($p < 10^{-3}$ for $M = 6$). Obviously embayed craters are found on only ~30% of the surface, with a ~10% reduction in the local crater density, meaning that associated magmatism only represents ~3% of the total—reflecting a possibly distinct qualitative origin that nevertheless remains quantitatively minor in the grand scheme of the cratering record.

6. Discussion

Stagnant-lid convection involves two primary sources of magmatism that may correspond to our two models of resurfacing processes. Over time, mantle material rises to replace cold, sinking lithosphere. Pressure-release melting of this passively upwelling mantle could cause localized, thin flows on the surface, although the nature of extrusive volcanism related to this process requires further investigation [e.g., *Phillips and Hansen*, 1994; *Reese et al.*, 2007]. Plate tectonics concentrates pressure-release melting at spreading centers, but passive upwellings are widespread under stagnant lids, supporting our assumption of spatial uniformity for this type of resurfacing [e.g., *Solomatov and Moresi*, 2000; *Armann and Tackley*, 2012; *Noack et al.*, 2012]. Localized mobilization of near-surface lithosphere during periods of extremely high surface temperatures is an alternative source of these flows [*Noack et al.*, 2012].

Large shield volcanoes are possibly related to mantle plumes, particularly in areas that resemble terrestrial hot spots like Hawaii [e.g., *Smrekar et al.*, 2010]. Anomalously hot material rising from the core/mantle boundary drives a few (~9) plumes on Venus that are likely responsible for large volcanic rises, young flows, and associated emissivity anomalies [*Smrekar et al.*, 2010; *Smrekar and Sotin*, 2012]. Stagnant-lid convection

is inefficient compared to plate tectonics, so a well-insulated mantle may initially limit core cooling. Passive upwelling may have produced more magmatism on Mars than mantle plumes until ~1–2 Ga [*Weizman et al.*, 2001]. Likewise, plumes inside Venus are perhaps a recent phenomenon, whereas magmatism from passive upwelling has continued throughout geologic time. The duration and dynamics of plume activity, however, are sensitive to poorly determined properties of the interior of Venus [e.g., *Smrekar and Sotin*, 2012].

Higher resolution imagery and topography are required to better constrain our models. For example, we predict that dark-floored craters exhibit a wide spectrum of rim-floor depths and rim heights, implying degrees of volcanic flooding ranging from negligible to nearly complete. Analysis of the limited sample of craters with stereo-derived topography suggests but does not confirm this hypothesis [*Herrick and Rumpf*, 2011]. There is a well-known correlation between the locations of obviously embayed craters and large volcanic edifices, particularly in the Beta-Atla-Themis region [e.g., *Herrick and Phillips*, 1994; *Strom et al.*, 1994; *Crumpler et al.*, 1997]. Future data and mapping, however, might reveal that some obviously embayed craters are associated with other processes like multiple thin flows, instead of shield volcanoes. Most dark-floored craters are located on the plains, which generally lack obvious volcanic sources [e.g., *Ivanov and Head*, 2013].

7. Conclusions

Early studies of the cratering record on Venus birthed the catastrophic resurfacing hypothesis, bolstered later by the directional stratigraphic history. But new evidence that the dark-floored craters have suffered postimpact volcanic modification potentially violates the fundamental assumption made by those initial investigations that most craters on Venus are pristine. Our Monte Carlo simulations demonstrate that two types of noncatastrophic volcanism can explain the observed cratering record. We reproduce the modern spatial and size-frequency distributions of dark-floored craters using a model featuring thin, morphologically similar flows that escape from vents spread over a wide area and penetrate rims at short length scales or fill craters from vents that open on their floors. Large shield volcanoes associated with a limited amount of hot spot magmatism or another geologic process are possibly responsible for the clustered population of obviously embayed craters. Improved imagery and topography are required to definitively link modified craters to volcanic sources.

Acknowledgments

The corresponding author will provide all data and code used for this study on request. The original LPI and USGS databases of impact craters on Venus are available for download from the websites of their host institutions. J.G. O'Rourke is supported by a National Science Foundation Graduate Research Fellowship. We thank S. Smrekar and R. Phillips for extremely constructive reviews.

The Editor thanks Roger Phillips and Suzanne Smrekar for their assistance in evaluating this paper.

References

Agnor, C. B., R. M. Canup, and H. F. Levison (1999), On the character and consequences of large impacts in the late stage of terrestrial planet formation, *Icarus*, *142*(1), 219–237, doi:10.1006/icar.1999.6201.

Armann, M., and P. J. Tackley (2012), Simulating the thermochemical magmatic and tectonic evolution of Venus's mantle and lithosphere: Two-dimensional models, *J. Geophys. Res.*, *117*, E12003, doi:10.1029/2012JE004231.

Basilevsky, A. T., and J. W. Head (1998), The geologic history of Venus: A stratigraphic view, *J. Geophys. Res.*, *103*(E4), 8531–8544, doi:10.1029/98JE00487.

Basilevsky, A. T., and J. W. Head (2000), Geologic units on Venus: Evidence for their global correlation, *Planet. Space Sci.*, *48*(1), 75–111, doi:10.1016/S0032-0633(99)00083-5.

Basilevsky, A. T., and J. W. Head (2002), Venus: Timing and rates of geologic activity, *Geology*, *30*(11), 1015–1018, doi:10.1130/0091-7613(2002)030<1015:VTAROG>2.0.CO;2.

Bjonnes, E., V. Hansen, B. James, and J. Swenson (2012), Equilibrium resurfacing of Venus: Results from new Monte Carlo modeling and implications for Venus surface histories, *Icarus*, *217*(2), 451–461, doi:10.1016/j.icarus.2011.03.033.

Bullock, M., and D. H. Grinspoon (2001), The recent evolution of climate on Venus, *Icarus*, *150*(1), 19–37, doi:10.1006/icar.2000.6570.

Collins, G. C., J. W. Head, A. T. Basilevsky, and M. A. Ivanov (1999), Evidence for rapid regional plains emplacement on Venus from the population of volcanically embayed impact craters, *J. Geophys. Res.*, *104*(E10), 24,121–24,140, doi:10.1029/1999JE001041.

Crumpler, L. S., J. C. Aubele, D. A. Senske, S. T. Keddie, K. P. Magee, and J. W. Head (1997), Volcanoes and centers of volcanism on Venus, in *Venus II*, edited by S. W. Bougher, a. D. M. Hunten, and R. J. Phillips, pp. 697–756, Arizona Univ. Press, Tucson, Ariz.

Guest, J., and E. R. Stofan (1999), A new view of the stratigraphic history of Venus, *Icarus*, *139*(1), 55–66, doi:10.1006/icar.1999.6091.

Hansen, V., and I. Lopez (2010), Venus records a rich early history, *Geology*, *38*(4), 311–314, doi:10.1130/G30587.1.

Hauck, S. A., R. J. Phillips, and M. H. Price (1998), Venus: Crater distribution and plains resurfacing models, *J. Geophys. Res.*, *103*(E6), 13,635–13,642, doi:10.1029/98JE00400.

Head, J. W., L. S. Crumpler, J. C. Aubele, J. E. Guest, and R. S. Saunders (1992), Venus volcanism: Classification of volcanic features and structures, associations, and global distribution from Magellan data, *J. Geophys. Res.*, *13*(E8), 13,153–13,197, doi:10.1029/92JE01273.

Herrick, R., and R. J. Phillips (1994), Implications of a global survey of Venusian impact craters, *Icarus*, *111*(2), 387–416, doi:10.1006/icar.1994.1152.

Herrick, R. R., and M. E. Rumpf (2011), Postimpact modification by volcanic or tectonic processes as the rule, not the exception, for Venusian craters, *J. Geophys. Res.*, *116*, E02004, doi:10.1029/2010JE003722.

Herrick, R. R., and V. L. Sharpton (2000), Implications from stereo-derived topography of Venusian impact craters, *J. Geophys. Res.*, *105*(E8), 20,245–20,262, doi:10.1029/1999JE001225.

Herrick, R. R., V. L. Sharpton, M. C. Malin, S. N. Lyons, and K. Feely (1997), Morphology and morphometry of impact craters, in *Venus II*, edited by S. W. Bougher, a. D. M. Hunten, and R. J. Phillips, pp. 1015–1046, Arizona Univ. Press., Tucson, Ariz.

Ivanov, M. A., and J. W. Head (2011), Global geological map of Venus, *Planet. Space Sci.*, *59*(13), 1559–1600, doi:10.1016/j.pss.2011.07.008.
Ivanov, M. A., and J. W. Head (2013), The history of volcanism on Venus, *Planet. Space Sci.*, *84*, 66–92, doi:10.1016/j.pss.2013.04.018.
Izenberg, N. R., R. E. Arvidson, and R. J. Phillips (1994), Impact crater degradation on Venusian plains, *Geophys. Res. Lett.*, *21*(4), 289–292, doi:10.1029/94GL00080.
Korenaga, J. (2010), On the likelihood of plate tectonics on Super-Earths: Does size matter?, *Astrophys. J. Lett.*, *725*(1), L43–L46, doi:10.1088/2041-8205/725/1/L43.
Korenaga, J. (2012), Plate tectonics and planetary habitability: Current status and future challenges, *Ann. N.Y. Acad. Sci.*, *1260*, 87–94, doi:10.1111/j.1749-6632.2011.06276.x.
McKinnon, W. B., K. J. Zhanle, B. D. Ivanov, and J. H. Melosh (1997), Cratering on Venus: Models and observations, in *Venus II*, edited by S. W. Bougher, a. D. M. Hunten, and R. J. Phillips, pp. 969–1014, Arizona Univ. Press, Tucson, Ariz.
Moresi, L., and V. Solomatov (1998), Mantle convection with a brittle lithosphere: Thoughts on the global tectonic styles of the Earth and Venus, *Geophys. J. Int.*, *133*(3), 669–682, doi:10.1046/j.1365-246X.1998.00521.x.
Namiki, N., and S. C. Solomon (1998), Volcanic degassing of argon and helium and the history of crustal production on Venus, *J. Geophys. Res.*, *103*(E2), 3655–3677, doi:10.1029/97JE03032.
Noack, L., D. Breuer, and T. Spohn (2012), Coupling the atmosphere with interior dynamics: Implications for the resurfacing of Venus, *Icarus*, *217*(2), 484–498, doi:10.1016/j.icarus.2011.08.026.
O'Rourke, J. G., and J. Korenaga (2012), Terrestrial planet evolution in the stagnant-lid regime: Size effects and the formation of self-destabilizing crust, *Icarus*, *221*(2), 1043–1060, doi:10.1016/j.icarus.2012.10.015.
Phillips, R. J., and V. L. Hansen (1994), Tectonic and magmatic evolution of Venus, *Annu. Rev. Earth Planet. Sci.*, *22*(1), 597–656, doi:10.1146/annurev.ea.22.050194.003121.
Phillips, R. J., R. F. Raubertas, R. E. Arvidson, I. C. Sarkar, R. R. Herrick, N. Izenberg, and R. E. Grimm (1992), Impact craters and Venus resurfacing history, *J. Geophys. Res.*, *97*(E10), 15,923–15,948, doi:10.1029/92JE01696.
Reese, C., V. Solomatov, and L. Moresi (1999), Non-Newtonian stagnant lid convection and magmatic resurfacing on Venus, *Icarus*, *80*, 67–80.
Reese, C. C., V. S. Solomatov, and C. P. Orth (2007), Mechanisms for cessation of magmatic resurfacing on Venus, *J. Geophys. Res.*, *112*, E04S04, doi:10.1029/2006JE002782.
Romeo, I. (2013), Monte Carlo models of the interaction between impact cratering and volcanic resurfacing on Venus: The effect of the Beta-Atla-Themis anomaly, *Planet. Space Sci.*, *87*, 157–172, doi:10.1016/j.pss.2013.07.010.
Schaber, G. G., R. G. Strom, H. J. Moore, L. A. Soderblom, R. L. Kirk, D. J. Chadwick, D. D. Dawson, L. R. Gaddis, J. M. Boyce, and J. Russell (1992), Geology and distribution of impact craters on Venus: What are they telling us?, *J. Geophys. Res.*, *97*(E8), 13,257–13,301, doi:10.1029/92JE01246.
Schultz, P. H., and P. D. Spudis (1983), Beginning and end of lunar mare volcanism, *Nature*, *302*(5905), 233–236, doi:10.1038/302233a0.
Scott, D., and C. Tout (1989), Nearest neighbour analysis of random distributions on a sphere, *Mon. Not. R. Astron. Soc.*, *241*, 109–117.
Smrekar, S. E., and C. Sotin (2012), Constraints on mantle plumes on Venus: Implications for volatile history, *Icarus*, *217*(2), 510–523, doi:10.1016/j.icarus.2011.09.011.
Smrekar, S. E., E. R. Stofan, N. Mueller, A. Treiman, L. Elkins-Tanton, J. Helbert, G. Piccioni, and P. Drossart (2010), Recent hotspot volcanism on Venus from VIRTIS emissivity data, *Science*, *328*(5978), 605–608, doi:10.1126/science.1186785.
Solomatov, V. S. (1995), Scaling of temperature- and stress-dependent viscosity convection, *Phys. Fluids*, *7*(2), 266, doi:10.1063/1.868624.
Solomatov, V. S., and L.-N. Moresi (1996), Stagnant lid convection on Venus, *J. Geophys. Res.*, *101*(E2), 4737–4753, doi:10.1029/95JE03361.
Solomatov, V. S., and L.-N. Moresi (2000), Scaling of time-dependent stagnant lid convection: Application to small-scale convection on Earth and other terrestrial planets, *J. Geophys. Res.*, *105*(B9), 21,795–21,818, doi:10.1029/2000JB900197.
Stofan, E., A. Brian, and J. Guest (2005), Resurfacing styles and rates on Venus: Assessment of 18 Venusian quadrangles, *Icarus*, *173*(2), 312–321, doi:10.1016/j.icarus.2004.08.004.
Strom, R., G. Schaber, and D. Dawson (1994), The global resurfacing of Venus, *J. Geophys. Res.*, *99*, 10,899–10,926, doi:10.1029/94JE00388.
Turcotte, D. L. (1993), An episodic hypothesis for Venusian tectonics, *J. Geophys. Res.*, *98*(E9), 17,061–17,068, doi:10.1029/93JE01775.
Weizman, A., D. J. Stevenson, D. Prialnik, and M. Podolak (2001), Modeling the volcanism on Mars, *Icarus*, *150*(2), 195–205, doi:10.1006/icar.2000.6572.
Wichman, R. W. (1999), Internal crater modification on Venus: Recognizing crater-centered volcanism by changes in floor morphometry and floor brightness, *J. Geophys. Res.*, *104*(E9), 21,957–21,977, doi:10.1029/1997JE000428.